J Therm Anal Calorim (2012) 107:797–807
DOI 10.1007/s10973-011-1441-9

Re-investigation of the La–Mg phase diagram

Alexandre Berche · Pierre Benigni · Jacques Rogez · Marie-Christine Record

Received: 14 December 2010 / Accepted: 7 March 2011 / Published online: 2 April 2011

Abstract Literature results on the La–Mg binary system are critically reviewed. It is shown that most recent experimental results are not in agreement with the previously published assessments of the system. Thus, an experimental re-investigation of this phase diagram is required. Several alloys are synthesized from pure constitutive elements and characterized using X-ray diffraction, scanning electron microscopy, and differential thermal analysis. This study clarifies the phase equilibria in the La–Mg system. These results combined with the recent study of the enthalpies of formation of the intermediate compounds of this system provide a sound basis for the Calphad optimization of the system.

Keywords Lanthanum · Magnesium · Phase diagram · Differential thermal analysis

Introduction

Because of their low densities, magnesium-based alloys are very attractive for the transport industry. However, their mechanical characteristics are weak and the improvement of these properties requires the use of additive elements. It has already been shown in literature that addition of zinc and rare earths (RE) can strongly improve these properties [1–3]. Thus, the study of the RE–Mg–Zn systems arouses interest.

A. Berche (✉) · P. Benigni · J. Rogez · M.-C. Record
CNRS, IM2NP (UMR 6242), Aix-Marseille Université, FST Saint-Jérôme, Av. Escadrille Normandie Niémen—Case 251, 13397 Marseille Cedex, France
e-mail: alexandre.berche@gmail.com

The determination of the most pertinent composition for these alloys and the optimization of their processing conditions both rely on the good knowledge of the corresponding ternary phase diagrams and of its constitutive binaries.

Two distinct routes can be used to establish phase diagrams: the first one is to determine the equilibria by direct measurements; the second one is to measure thermodynamic properties of the system allowing to the calculation of the corresponding equilibria. The Calphad method uses all the available experimental results to give a global thermodynamic description of a multi-component system.

The aim of this study is to complete and clarify the available set of phase diagram data on the La–Mg system for subsequent optimization by the Calphad method.

Literature data

Several experimental studies of La–Mg phase diagram are reported in literature [4–10]. Three assessments of the system were also performed in the last years [11–13], however, since no original experimental data are presented in these studies, these articles are not taken into account in this article.

All the investigations of the La–Mg phase diagram were undertaken under normal pressure. Table 1 gathers the ranges of temperature and composition investigated in these studies as well as the methods used.

The experimental method of Vogel et al. [6] is not clearly described. The authors quote the utilization of thermal method, microscopic observation, and probably X-ray diffraction (XRD) method. The samples seems to have been annealed and rapidly cooled at 60 K/min. Moreover, the fusion point of lanthanum was extrapolated

Table 1 Experimental studies reported in literature: temperature and composition ranges and method

Experimental method	Temperature range/K	Composition range x_{Mg}	References
Thermal analysis on cooling	776–1085	0.000–1.000	Canneri [4]
Thermal analysis on cooling; electrical measurements; X-ray diffraction	713–878	0.975–1.000	Weibke and Schmidt [5]
Thermal method on cooling; microscopic observation, XRD	773–1193	0.000–0.800	Vogel et al. [6]
XRD	573–817	0.010–0.094	Joseph and Gschneider [7]
Differential thermal analysis on heating and cooling (2.5, 5, and 10 K/min)	573–883	0.000–0.650	Manfrinetti and Gschneider [8]
Differential scanning calorimetry on heating	400–800	0.180	Herchenroeder et al. [9]
Differential thermal analysis on cooling (2–10 K/min)	773–1073	0.800–1.000	Giovannini et al. [10]
X-ray diffraction	853–889	0.9986–0.9993	Park et al. [22]
Resistivity measurements	573–893	0.99958–0.99998	Rohklin and Bochvar [23]
Differential thermal analysis	573–903	0.960	Dobatkina et al. [24]

from the liquidus curve determined for $x_{Mg} = 0.15$–0.25 perhaps at too fast cooling rates. Since the fusion point of pure metal is not directly measured, it is not possible to estimate the accuracy of these measurements. Moreover, the purity of the elements is not quoted. The experimental results of Vogel et al. must be taken under consideration with a great care, especially concerning liquidus measurements.

The La–Mg phase diagram suggested by Massalski [14] is presented in Fig. 1. It corresponds to the assessment of the La–Mg phase diagram performed in 1988 by Nayeb-Hashemi and Clark [15]. This phase diagram contains five intermediate compounds: LaMg, $LaMg_2$, $LaMg_3$, La_2Mg_{17}, and $LaMg_{12}$. $LaMg_2$ only exists at high temperatures, between 998 and 1048 K according to [15]; the other phases are reported to be stable from room temperature up to their melting or decomposition points.

The Mg-rich region was further subsequently re-investigated [10] showing the existence of an additional intermediate phase La_5Mg_{41}.

The intermediate phases

- LaMg ($x_{Mg} = 0.5$) crystallizes into a CsCl-type structure, space group Pm-3m [16]. Manfrinetti and Gschneider [8] investigated the lanthanum solubility into this phase and found it negligible. LaMg undergoes peritectic decomposition at 1018 K [6, 8]. The corresponding reaction on cooling is [liquid + $LaMg_2$ = LaMg].
- A Laves phase $LaMg_2$ ($x_{Mg} = 0.667$; $MgCu_2$-type, space group cF24 was first described by Laves [17]. On cooling from the liquid, this phase crystallizes by the peritectic reaction: [liquid + $LaMg_3$ = $LaMg_2$]. The

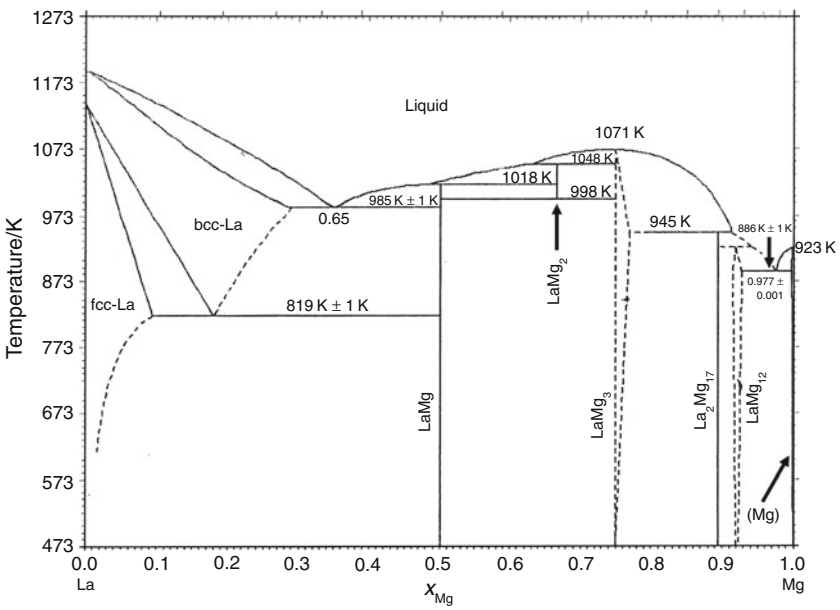

Fig. 1 La–Mg phase diagram from Massalski [14]

peritectic temperatures determined by Vogel et al. [6] and Manfrinetti and Gschneider [8] are in relative agreement: 1048 and 1053 K, respectively. As the temperature is lowered, this phase decomposes by the eutectoid reaction [$LaMg_2 = LaMg + LaMg_3$] at 998 K according to Manfrinetti and Gschneider [8] or at 899 K according to Vogel et al. [6].

- The cubic phase $LaMg_3$ ($x_{Mg} = 0.75$) isomorphic to BiF3 (cF16) is the only phase in the system exhibiting congruent melting at 1071 K depending to Vogel et al. [6] and to Giovannini et al. [10]. However, this temperature was measured in these two studies on cooling, an undercooling of a few Kelvin could occur. According to Vogel et al. [6], the solubility ranges from $x_{Mg} = 0.750$ to an upper limit of $x_{Mg} = 0.799$ at 948 K.
- The existence of the RE_5Mg_{41} ($x_{Mg} = 0.891$) phases (where RE = Ce, Pr, Nd, and Sm) lead Giovannini et al. [10] to investigate for the La_5Mg_{41} phase. This phase is tetragonal (tI92) isomorphic to Ce_5Mg_{41}. XRD measurements performed on a sample at $x_{Mg} = 0.891$ annealed 125 h at 873 K by Giovannini et al. [10] show the existence of La_5Mg_{41} in the La–Mg system. Thermal analyses do not permit to discriminate the decomposition temperature of the phases La_2Mg_{17} and La_5Mg_{41}. These two temperatures are probably very close. De Negri et al. [18] assume that this phase decomposes by eutectoid reaction below 873 K.
- The hexagonal phase La_2Mg_{17} ($x_{Mg} = 0.895$, isomorphic to $Ni_{17}Th_{12}$) was evidenced by Evdokimenko and Kripkyakevich [19]. It crystallises by a peritectic reaction [liquid + $La_5Mg_{41} = La_2Mg_{17}$] at 945 K depending to Giovannini et al. [10] or [liquid + $LaMg_3 = La_2Mg_{17}$] according to Vogel et al. [6]. Further analysis in the composition range from $x_{Mg} = 0.85$–0.90 could enlighten this region of the phase diagram.
- The richest magnesium phase of this system is the orthorhombic $LaMg_{12}$ ($x_{Mg} = 0.923$). Its crystalline structure presents a multiple cell, pseudo quadratic depending to Darriet et al. [20]. XRD analysis performed by Darriet et al. [20] on three alloys with composition ratios x_{La}/x_{Mg} equal to 1/11, 1/12, and 1/13 annealed at 903 K prior to quenching show that a composition range of the $LaMg_{12}$ phase could exist from $x_{Mg} = 0.917$ to 0.929. More recently, Denys et al. [21] resolves the crystal structure by synchrotron XRD. The orthorhombic phase is described with a giant unit cell. The space group is Immm built from the altered layers of the $ThMn_{12}$-type structure. A substantial deviation to the ideal stoichiometry could occurs from Mg/La = 12 down to Mg/La = 10.857. The $LaMg_{12}$ phase crystallises into the peritectic transition [liquid + $La_2Mg_{17} = LaMg_{12}$] on cooling at 913 K depending to Giovannini et al. [10].

The stability ranges of the intermediate phases and their crystallographic data are gathered in Table 2.

The solid solutions : dhcp-La, bcc-La, fcc-La, and hcp-Mg

The solubilities of lanthanum in hcp-Mg was previously discussed by Nayeb-Hashemi and Clark [15]. The results

Table 2 Range of stability and crystallographic data of the intermediate phases of the La–Mg system

Phase	Range of stability		Crystal structure			Cell parameters/Å			Reference
	x_{Mg}	T/K	Space group	Pearson symbol	Prototype	*a*	*b*	*c*	
LaMg	0.500	–	*P*3−3*m*	cP2	CsCl	3.96	–	–	[16]
	0.500	<1018	–	–	–	–	–	–	[6]
	0.500	<1018	–	–	–	–	–	–	[8]
$LaMg_2$	0.667	–	*Fd*−3*m*	cF24	$MgCu_2$	8.79	–	–	[17]
	–	899–1048	–	–	–	–	–	–	[6]
	–	998–1053	–	–	–	–	–	–	[8]
$LaMg_3$	–	–	*Fm*−3*m*	cF16	BiF_3	7.45–7.47	–	–	[16]
	0.750–0.799	1071	–	–	–	–	–	–	[6]
	–	1071	–	–	–	–	–	–	[10]
La_5Mg_{41}	0.891	873–943	I4/*m*	tI92	Ce_5Mg_{41}	14.82	–	10.47	[10]
	0.891	873–943	–	–	–	–	–	–	[18]
La_2Mg_{17}	0.895	–	$P6_3/mmc$	hP38	$Ni_{17}Th_{12}$	10.35	–	10.25	[19]
	0.895	<945	–	–	–	–	–	–	[10]
$LaMg_{12}$	0.917–0.929	<913	I4/*mmm*	oI238	$ThMn_{12}$	10.32– 10.37	10.32– 10.37	77.24–77.56	[20]
	0.923	–	–	–	–	–	–	–	[10]
	0.916–0.923	–	*Immm*	–	$ThMn_{12}$	10.3391(5)	10.3554(5)	77.484(4)	[21]

obtained by Park et al. [22] were preferred to those obtained by Rokhlin and Bochvar [23] or Weibke and Schmidt [5]. Since no further solubility measurements were performed concerning these solids solutions, the conclusions of Nayeb-Hashemi and Clark will be used in this study. Solubility of magnesium in bcc-La was measured by Manfrinetti and Gschneider [8] by DTA measurements. The solvus curve involving fcc-La was determined by Manfrinetti and Gschneider [8] for temperature higher than 900 K by differential thermal analysis (DTA) on heating and by Joseph and Gschneider [7] for T < 850 K using X-ray parametric technique.

The invariant reactions

Twelve invariant reactions can be listed from literature data. They are detailed in Table 3. In addition to the reactions mentioned in the previous paragraph which correspond to the formation and the decomposition of the intermediate solid phases, an eutectoid and a peritectoid reaction derivate from allotropic reactions of the lanthanum and two others eutectic reactions were reported. The additional equilibria on cooling are as follows:

- The peritectoid [fcc-La + LaMg = dhcp-La] was measured at 603 ± 2 K by Herchenroeder et al. [9] by thermal analysis performed on an alloy at $x_{Mg} = 0.18$ heated at 10 K/min. No other indications are available for this equilibrium.
- The eutectoid [bcc-La = fcc-La + LaMg] has been detected at 803 K on cooling by Vogel et al. [6], and at 819 K on heating by Manfrinetti and Gschneider [8]. The composition of the bcc-La phase involved in the ternary equilibrium is estimated at $x_{Mg} = 0.25$ by Vogel et al. and at $x_{Mg} = 0.184$ by Manfrinetti. This last value is obtained from metallographic analysis of four alloys ($x_{Mg} = 0.149$, 0.164, 0.183, and 0.200) annealed 4 days at 833 K prior to quenching. The results of Manfrinetti and Gschneider [8] are preferred because of the method involved.
- The eutectic reaction [liquid = bcc-La + LaMg] occurs at 968 K according to Vogel et al. [6] and at 985 K according to Manfrinetti and Gschneider [8]. The composition of the liquid involved is estimated at

Table 3 Invariant reactions in the La–Mg system

Equilibrium on cooling	Reaction type	x_{Mg} of the phases involved			Temperature/K	References
fcc-La + LaMg = dhcp-La	Peritectoïd	–	0.500	–	603 ± 2	[9]
bcc-La = fcc-La + LaMg	Eutectoïd	0.250	–	0.500	803	[6]
		0.184	0.080	0.500	819	[8]
Liquid = bcc-La + LaMg	Eutectic	0.388	–	0.500	968	[6]
		0.350	0.300	0.500	985	[8]
Liquid + $LaMg_2$ = LaMg	Peritectic	–	0.667	0.500	1018	[6]
		–	0.667	0.500	1018	[8]
		–	0.667	0.500	994 ± 5	This study
$LaMg_2$ = LaMg + $LaMg_3$	Eutectoïd	0.667	0.500	0.750	899	[6]
		0667	0.500	0.750	998	[8]
Liquid + $LaMg_3$ = $LaMg_2$	Peritectic	–	0.750	0.667	1048	[6]
		–	0.750	0.667	1053	[8]
		–	0.750	0.667	1040 ± 4	This study
Liquid = $LaMg_3$	Congruent	0.750	0.750	–	1071	[6] [10]
La_5Mg_{41} = La_2Mg_{17} + $LaMg_3$	Eutectoid	0.891	0.895	0.750	< 873	[18]
		0.891	0.895	0.750	> 850	This study
$LaMg_3$ + liquid = La_2Mg_{17}	Peritectic	0.799	–	0.895	945	[6]
$LaMg_3$ + liquid = La_5Mg_{41}	Peritectic	0.750	–	0.891	943	[18]
		0.750	–	0.891	948 ± 5	This study
Liquid + La_5Mg_{41} = La_2Mg_{17}	Peritectic	–	0.891	0.895	947	[10]
		–	0.891	0.895	942 ± 2	This study
La_2Mg_{17} + liquid = $LaMg_{12}$	Peritectic	0.895	–	0.923	913	[10]
		0.895	–	0.923	925 ± 3	This study
Liquid = hcp-Mg + ($LaMg_{12}$)	Eutectic	0.977	–	0.923	883	[5]
		0.977	–	–	883	[10, 24]
		–	–	0.923	885 ± 1	This study

$x_{Mg} = 0.388$ [6] or $x_{Mg} = 0.350$. For the same lanthanum purity argument, the results of Manfrinetti and Gschneider [8] are preferred.

- The eutectic reaction [liquid = hcp-Mg + $LaMg_{12}$] was observed at 883 K by Weibke and Schmidt [5], Giovannini et al. [10], and by Dobatkina et al. [24]. The composition of the liquid phase was estimated between $x_{Mg} = 0.977$ and 0.978.

The liquidus curves

The liquidus points reported in literature are presented in Fig. 2.

The first liquidus measurements were performed by Canneri [4]. However, their data do not agree with those published more recently and they found a melting point of lanthanum which is 110 K lower than the accepted SGTE value [25]. Thus, Canneri's data do not seem reliable.

Later on, Vogel et al. [6] measured the liquidus in the composition range $x_{Mg} = 0.0$–0.80. Nevertheless, as already mentioned, Vogel's results concerning liquidus curve must be considered with caution because of the experimental method involved.

Manfrinetti and Gschneider [8] reported liquidus points between $x_{Mg} = 0.00$ and $x_{Mg} = 0.65$. Their values are in agreement with those reported by Vogel et al. for samples with compositions above $x_{Mg} = 0.50$.

For compositions ranging from $x_{Mg} = 0.95$–1.00, the shape of the liquidus determined on cooling by Weibke and Schmidt [5] indicates a tendency to demixtion in the liquid. Giovannini et al. [10] estimated the liquidus temperatures on cooling. Their value is 10 K lower than those reported by Weibke and Schmidt.

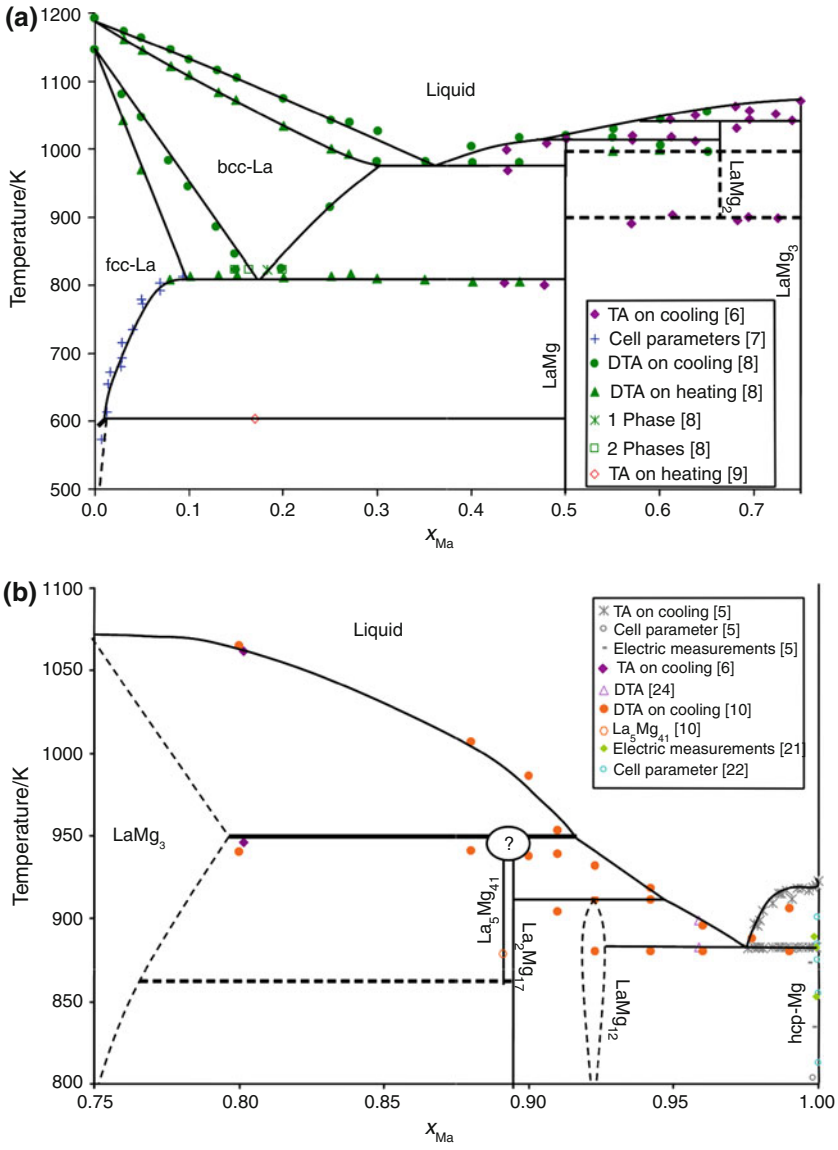

Fig. 2 The La–Mg phase diagram from experimental literature data: **a** composition range from $x_{Mg} = 0.00$–0.75; **b** composition range from $x_{Mg} = 0.75$–1.00

This literature review has highlighted several discrepancies in the phase diagram. They concern the temperature stability range of $LaMg_2$ and the existence of La_5Mg_{41}. If this latter phase exists, its stability range needs to be defined and the melting reaction of La_2Mg_{17} needs to be clarified.

These points are re-investigated experimentally in this study in order to provide a reliable phase diagram for further Calphad calculations.

Experiments

Elaboration of the samples

Several alloys were synthesized from the pure constitutive elements, La and Mg, weighed in stoichiometric ratios.

The purity of the elements are as follows: La ($x_{La} > 0.999$, Huhhot Jinrui Rare Earth Co. Ltd) and Mg shots ($x_{Mg} = 0.9998$, Aldrich). Both magnesium and lanthanum were handled in a glove box to prevent oxidation (<1 ppm O_2, <20 ppm H_2O). Before weighing, the oxide layer covering the lanthanum pieces was mechanically removed.

Tantalum crucibles (18 mm in diameter and 11 mm in height) used in this study were cold-stamped from a tantalum sheet with a thickness of 0.25 mm and supplied by Technicome. They were filled in and sealed by Tungsten Inert Gas welding, under argon atmosphere in a glove box.

Samples were then heated up to 1,250 K for 10 min to get a homogeneous liquid alloy, and then annealed in the solid state to reach equilibrium. The annealing conditions are detailed in Table 4.

The samples are called LaX–MgY where X and Y correspond to $100 \times x_{Mg}$ and $100 \times x_{La}$, respectively. The sample La33–Mg67 was first annealed at 1029 K for 100 h and then rapidly quenched to 298 K in oil bath. Following this treatment, this sample was cut into two pieces : the first one, called La33–Mg67–HT, was directly characterized; the second one was submitted to an additional annealing at 836 K for 170 h before being characterized and will hereafter be called La33–Mg67–LT. The sample La15–Mg85–HT was annealed at 850 K for 150 h prior to oil quenching.

Characterization of the samples

The alloys were characterized by XRD, scanning electron microscopy (SEM), and DTA.

Phases identification: XRD and SEM

The diffraction patterns were recorded on a Philips Expert diffractometer (with a copper $K_{\alpha 1}$ anticathode) in the [10–100°] 2θ range, with a step size of 0.01671° and a step time of 130 s.

The lattice parameters were determined from these diffraction patterns using the Powdercell program [26]. From the crystal structure of a phase, Powdercell calculates its theoretical pattern and by using a refinement algorithm, this program determines the lattice parameter(s) corresponding to the experimental diffraction pattern.

SEM measurements were performed on a FEG XL30S—Oxford Instruments. This Scanning Electron Microscope is equipped with an Energy Dispersive X-ray spectroscope which allows the quantitative analysis of the phase compositions.

Differential thermal analysis (DTA)

DTA is performed in a high temperature furnace (<1700 K). In order to prevent crucible oxidation, the

Table 4 Composition, annealing conditions, XRD and SEM results on the samples

Alloy	x_{Mg}	Annealing	Phases		Cell parameters/Å		References
		T/K/duration/h	SEM	XRD	This study	Literature	
La50-Mg50	0.500	850/100	LaMg	LaMg	3.97	3.96	[16]
La33-Mg67-HT	0.667	1029/100	$LaMg_2$	$LaMg_2$	8.79	8.79	[17]
La33-Mg67-LT	0.667	836/170	–	$LaMg_2$	8.78	8.79	[17]
			–	$LaMg_3$	7.48	7.45–7.47	[16]
			–	LaMg	3.99	3.96	[16]
La25-Mg75	0.750	840/100	$LaMg_3$	$LaMg_3$	7.48	7.45–7.47	[16]
La15-Mg85-HT	0.850	850/150	–	$LaMg_3$	7.46	7.45–7.47	[16]
			–	La_2Mg_{17}	$a = 10.37$ $c = 10.22$	$a = 10.365$ $c = 10.244$	[19]
La10-Mg90	0.895	840/213	–	La_2Mg_{17}	$a = 10.37$ $c = 10.22$	$a = 10.365$ $c = 10.244$	[19]
La08-Mg92	0.921	860/70	–	$LaMg_{12}$	–	$a = 10.32$–10.37	[10]
						$b = 10.32$–10.37	
						$c = 77.24$–77.56	

furnace is evacuated and then backfilled with 75 ± 5 mm Hg of argon. This process is repeated several times before starting the experiment. The rate of temperature change of the furnace is controlled between +15 K/min and −15 K/min (a negative value meaning here that the furnace is cooling down).

The DTA cell [27] used in this study has two main features. First, the design of the measurement cell and its location in the furnace is optimized to achieve very good thermal homogeneity of the whole assembly. The resulting thermal gradient between the reference and the sample crucible is null in the absence of transition in the sample. Second, some alumina shields prevent thermal leaks between the reference and the sample crucibles to achieve maximum sensitivity of the apparatus.

The sample is sealed under argon in tantalum crucibles using the method described earlier. The size of the DTA crucibles is 8 mm in diameter and 5–6 mm in height. S-type thermocouples in Pt/Pt-Rh 10% are used. The cold junction of the thermocouples is controlled at 40 ± 0.1 °C. The reference crucible is kept empty.

The electric signals corresponding to the temperature of the sample and the temperature difference between the two crucibles are measured and digitalized by a Keithley nanovoltmeter (2182 model) and recorded on a microcomputer.

For each sample, DTA runs are performed at various heating and cooling rates in order to interpolate the temperature at thermodynamical equilibrium or null rate.

It was not possible to calibrate the measuring chain toward classical metallic standards such as gold or silver, because of their reactivity with tantalum. However, the melting temperature of four pure metals (tin, zinc, magnesium, and lanthanum) has been verified.

Results and discussion

Identification of the phases

Results obtained by SEM and XRD are presented in Table 4. The lattice parameters obtained for each phase are compared to those reported in literature. The results are in good agreement with literature data within a maximum error of ±0.35%.

The variation of the measured parameter for the $LaMg_3$ phase measured in the samples La33–Mg67–LT, La25–Mg75, and La15–Mg85–HT is consistent with the stoichiometry range of this phase measured by Vogel et al. [6]. Moreover, it is confirmed that the parameter decrease when x_{Mg} increase. Finally, the a value of 7.46 Å measured for the $LaMg_3$ in La15-Mg85-HT evidenced that at 850 K, the compound $LaMg_3$ still admit a variation to the stoichiometry.

As mentioned here, La33–Mg67–LT was obtained from La33–Mg67–HT after an annealing treatment at 836 K for 170 h. In agreement with the phase diagram reported in literature, La33–Mg67–HT is constituted of $LaMg_2$ and La33–Mg67-LT contains LaMg and $LaMg_3$. However, $LaMg_2$ is still present in the latter sample. This result suggests that an annealing at 836 K for 170 h is not sufficient to completely transform the $LaMg_2$ phase and to reach the equilibrium. The high temperature stability of $LaMg_2$ is confirmed.

The La15–Mg85–HT alloy was synthesized to check the stability range of La_5Mg_{41}. Giovannini et al. [10] evidenced this phase in a sample annealed at 873 K. Later on, De Negri et al. [18] suggested this phase to be stable above 873 up to 943 K. The results show that the La15–Mg85–HT sample annealed at 850 K for 150 h is made of $LaMg_3$ and La_2Mg_{17}. Then it can be concluded that the lower temperature bound of La_5Mg_{41} stability ranges from 850 to 873 K.

Phase transformations

The melting point of Sn, Zn, Mg, and La are measured (Table 5). These values are in very good agreement with the reference data selected by SGTE within the experimental uncertainty (<±2 K). At high temperature, the signal to noise ratio of the DTA thermograms decreases. As a consequence, the uncertainty on the transition temperature measurement increases. This phenomenon is particularly critical for weakly energetic solid/solid transitions. This can explain the higher uncertainties associated with the lanthanum values.

The phase transformation temperatures were determined for four binary alloys (LaMg, $LaMg_2$, La_2Mg_{17}, and $LaMg_{12}$). The results obtained at several heating and cooling rates are reported in Appendix and intrapolated at 0 K/min (Table 5).

The equilibrium temperatures for the four binary alloys are plotted with literature data in Fig. 3. Based on the results, a new phase diagram is drawn in the composition range $x_{Mg} = 0.85$–0.95.

The results confirm the peritectic decomposition observed for LaMg in [6] and [8]. However, the temperature determined in this study (994 K) is 24 K lower than that previously reported in literature (1018 K).

The similarity between the result (994 K) and that reported by Manfrinetti and Gschneider [8] for the eutectoid decomposition of $LaMg_2$ (998 K) is intriguing. Furthermore Vogel et al. [6] reported 899 K for this reaction. We were not able to detect this eutectoid transition on the La33–Mg67 sample using heating and cooling rate ranging from −0.7 to +12 K/min comparable to those used by Manfrinetti (2.5, 5, and 10 K/min). This phenomenon is consistent with the sluggish kinetics of the eutectoid

Table 5 Phase transformation temperatures from this study compared to those from literature

Sample	Temperature/K		Phase transformation on cooling
	This study	Literature	
Sn	505 ± 1	505 [25]	Liquid = bct-Sn
Zn	968 ± 2	966 [25]	Liquid = hcp-Zn
La	1200 ± 8	1193 [25]	Liquid = bcc-La
	1115 ± 15	1134 [25]	bcc-La = fcc-La
La50-Mg50	994 ± 5	1018 [6, 8]	Liquid + $LaMg_2$ = LaMg
	1016 ± 4	1020 [8]	Liquidus
La33-Mg67	1040 ± 4	1048 [6], 1053 [8]	Liquid + $LaMg_3$ = $LaMg_2$
	1048 ± 1	1060 [8]	Liquidus
La10-Mg90	942 ± 2	943 [10]	Liquid + La_5Mg_{41} = La_2Mg_{17}
	948 ± 5	945 [10]	Liquid + $LaMg_3$ = La_5Mg_{41}
La08-Mg92	885 ± 1	883 [5, 10, 24]	Liquid = $LaMg_{12}$ + hcp-Mg
	925 ± 3	913 [10]	Liquid + La_2Mg_{17} = $LaMg_{12}$
	942 ± 2	943 [10]	Liquid + La_5Mg_{41} = La_2Mg_{17}
Mg	924 ± 2	923 [25]	Liquid = Mg

reaction as only a partial transformation was observed by XRD analysis after 170 h at 836 K (Table 4). As a consequence, we may suggest that thermal scanning methods are unable to show this eutectoid transition and that the temperature assigned by Manfrinetti to the reaction of formation of $LaMg_2$ is in fact the temperature of the peritectic decomposition of LaMg. This experimental investigation is devoted to the pure line phases. DTA measurements and microanalysis on any additional samples as at $x_{Mg} = 0.45$ would be useful in a further study to confirm or infirm the nature of the decomposition of the LaMg compound.

The temperature of the reaction determinated by Vogel could be considered as reliable because of the experimental methods involved by the author, especially microscopic examination and XRD analysis performed on quenched alloys. Moreover, the temperature of 899 K measured by Vogel is in agreement with the three-phased alloy observed at 836 K on the sample La33–Mg67–HT in this study.

The liquidus temperature of LaMg determined in this study (1016 K) is in good agreement with the 1020 K reported by Manfrinetti and Gschneider [8].

The peritectic decomposition of $LaMg_2$ was evidenced in this study at 1040 ± 3 K. In contrast, higher values are reported in literature, namely 1048 K in [8] and 1053 K in [6]. A strong influence of the kinetics parameters on this decomposition is anticipated. In such situation, only the equilibrium temperature is valid. As already mentioned, this value can be reached by intrapolating at 0 K/min the temperatures observed at various rates. This also holds for the liquidus temperature which was recorded at 1069 K (see Appendix) at a rate of 12 K/min in this study. It means that for kinetics reasons, the study of the evolution of transition temperatures with the heating and cooling rates is an absolute necessity for accurate determination of the equilibrium values in this part of the phase diagram.

Two thermal effects were observed for La10–Mg90. The corresponding temperatures, 942 ± 2 and 948 ± 5 K, are in good agreement with those reported in [10] for the decomposition of La_2Mg_{17} and La_5Mg_{41}, respectively (see Table 5).

Three invariant temperatures were evidenced in the case of $LaMg_{12}$. In agreement with [10], the lowest one (885 ± 1 K) is attributed to the temperature of the eutectic reaction [liquid = $LaMg_{12}$ + hcp-Mg]. The detection of this invariant suggests that the magnesium content in the sample is slightly higher than the expected one. The second temperature (925 ± 2 K) could correspond to the peritectic decomposition of $LaMg_{12}$ [La_2Mg_{17} + liquid = $LaMg_{12}$] reported at 913 K by Giovannini et al. [10]. Since these authors determined the transition temperature on cooling, their lower value can be explained by an undercooling effect. The third invariant at 942 ± 2 K corresponds to the peritectic decomposition of La_2Mg_{17} [liquid + La_5Mg_{41} = La_2Mg_{17}]. This conclusion is also ascertained by the fact that the same transition temperature is measured for the samples La10–Mg90 and La08–Mg92.

In the cases of La10–Mg90 and La08–Mg92, the crossing of the liquidus curve was not detected. This could be due to a steep slope of this curve in the vicinity of these compositions.

The La–Mg phase diagram

The La–Mg phase diagram drawn from this study is plotted in Fig. 4. It results from a combination of a critical review

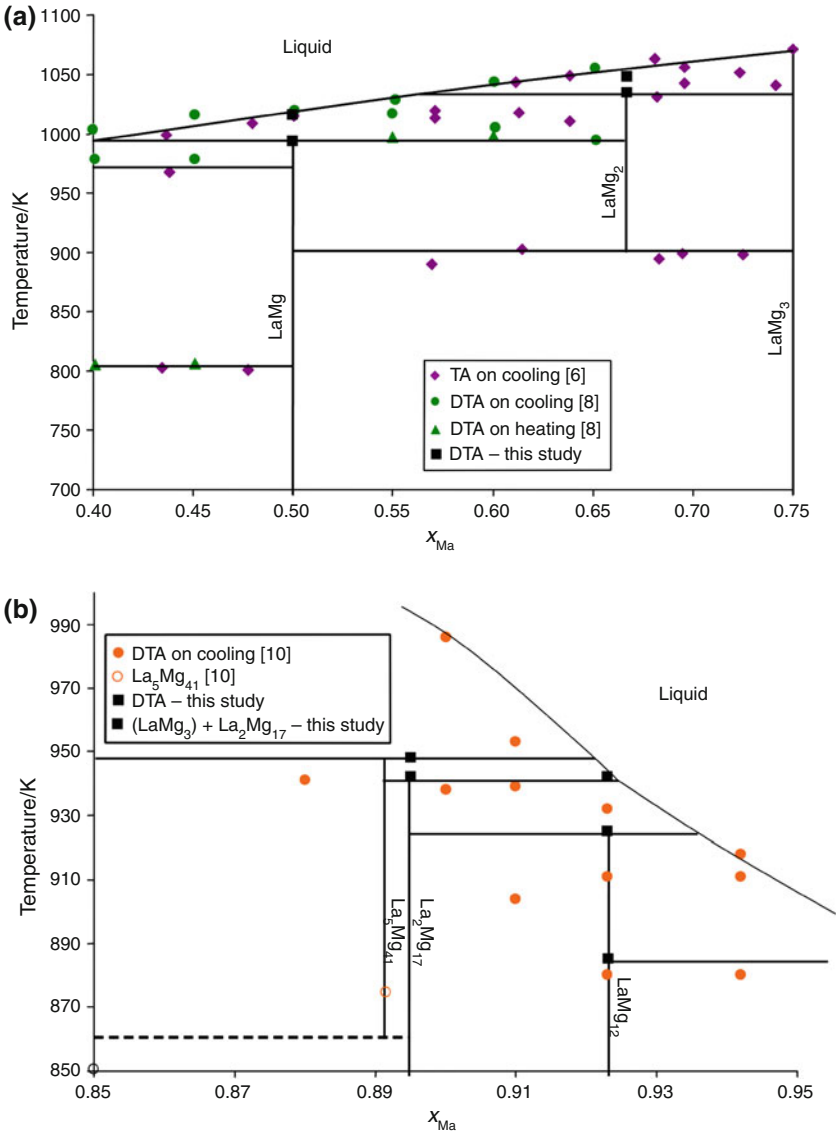

Fig. 3 Partial La-Mg phase diagram obtained in this study, compared to experimental literature data: **a** $x_{Mg} = 0.40$ to 0.75; **b** $x_{Mg} = 0.85$ to 0.95

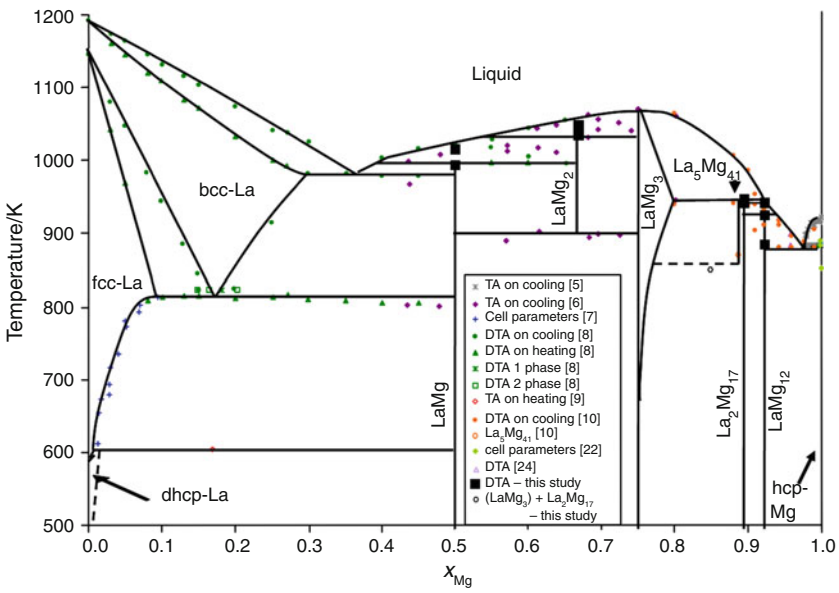

Fig. 4 La–Mg phase diagram from this study compared to selected experimental data

of literature data and new experimental results. The corresponding invariant reactions, compositions, and temperatures are listed in Table 3.

Conclusions

This study is based on a critical review of data literature of the La–Mg phase diagram and the new experimental investigations. The aim was to clarify the discrepancies encountered in literature and to suggest a reliable phase diagram for forthcoming Calphad calculations.

Assuming the existence of La_5Mg_{41} as suggested by Giovannini [10], its non-stability for $T < 850$ K is confirmed. The instability of the $LaMg_2$ phase at low temperatures was insured.

All the invariant temperatures are now clearly defined and assigned, in particular the melting temperatures of La_5Mg_{41} and La_2Mg_{17}.

Disagreements between the results previously reported were resolved and a new La–Mg phase diagram is presented. These phase diagram data, together with the measurements of enthalpy of formation of the intermediate compounds [28] provide a firm basis for the Calphad assessment of the La–Mg phase diagram. When combined to the results recently obtained on the La–Zn [29, 30] and Mg–Zn [31] systems, this study will allow a sound thermodynamic description of the ternary La–Mg–Zn system.

Appendix

See Table 6.

Table 6 Transition temperatures (T, in K) determined by DTA in the solid phases of the La-Mg system. These temperatures were determined with various heating and cooling rates (V, in K/min). V is positive for heating and negative for cooling. ΔT corresponds to the uncertainty

V	T	ΔT
La		
15.2	1130.3	5.7
−5.3	1131.7	4.2
7.8	1112.8	5.1
−3.8	1117.7	3.4
4.8	1103.6	7.7
−4.7	1112.9	3.5
15.2	1185.3	6.4
−5.3	1197.5	3.5
7.8	1197.1	6.6
−3.8	1206.5	3.2
4.8	1201.0	12.1
−4.7	1208.7	2.5
Mg		
10.2	924.9	1.7
−6.6	924.9	0.7
6.2	924.3	0.9
−4.7	925.5	0.2
3.8	925.2	1.3
−3.2	924.7	0.1
1.9	925.1	0.4
−1.7	923.5	0.2
LaMg		
7.6	999.2	2.6
3.3	996.4	2.0
−2.8	989.9	1.5
6.2	1027.9	1.3
−7.1	1016.3	1.3
7.6	1023.0	1.2
−5.9	1015.9	1.3
3.3	1016.7	0.1
−2.8	1011.4	0.7
$LaMg_2$		
−1.1	1045.6	0.3
4.6	1038.4	2.1
3.1	1036.3	2.1
1.6	1039.3	1.1
−0.7	1034.0	0.7
0.7	1043.3	1.0
12.0	1069.1	0.6
−5.6	1047.6	1.0
4.6	1054.3	1.3
−3.0	1044.7	1.3
3.1	1051.8	1.0
−2.2	1042.5	0.6
1.6	1049.1	0.6
−0.7	1043.0	0.6
0.7	1048.5	0.9
−1.1	1046.0	0.6
$LaMg_{12}$		
10.1	888.5	4.8
−9.9	883.7	1.4
12.2	887.0	1.7
−6.0	884.2	1.1
4.3	886.6	1.2
−2.8	884.8	0.5
10.1	933.9	0.8

Table 6 continued

V	T	ΔT
−9.9	926.7	1.3
12.2	928.9	2.4
−6.0	924.6	1.9
4.3	926.3	1.4
−2.8	922.2	1.5
10.1	956.6	1.5
−9.9	941.2	1.3
12.2	952.0	2.1
−6.0	941.7	2.0
4.3	946.4	1.7
−2.8	941.4	0.8
La_2Mg_{17}		
15.3	968.6	1.2
−8.6	946.8	1.2
6.1	957.9	0.9
−2.0	946.5	0.3
2.0	952.9	0.5
−0.9	945.9	0.5
15.3	949.9	1.6
6.1	946.4	0.9
−2.0	940.6	0.3
2.0	944.1	0.9

These temperatures were determined with various heating and cooling rates (V, in K/min), V is positive for heating and negative for cooling, and ΔT corresponds to the uncertainty

References

1. Wei LY, Dunlop GL, Westengen H. The intergranular microstructure of cast Mg-Zn and Mg-Zn-rare earth alloys. Metall Mater Trans A. 1995;26(8):1947–55.
2. Wei LY, Dunlop GL, Westengen H. Precipitation hardening of Mg-Zn and Mg-Zn-RE alloys. Metall Mater Trans A. 1995;26(7):1705–16.
3. Wu W, Wang Y, Zheng X, Chen LJ, Liu Z. Effect of neodynium on mechanical behavior of Mg-Zn-Zr magnesium alloy. J Mater Sci Lett. 2003;22(6):445–7.
4. Canneri G. Le leghe del lantanio. Metall Ital. 1931;23:803–23.
5. Weibke F, Schmidt W. Uber die Löslichkeit von Lanthan in Aluminium, Magnesium und den omogenen Legierungen des Magnesiums und Aluminiums. Z Electrochem. 1940;46:357–64.
6. Vogel VR, Heumann T. Berichtigung der Systeme Cer-Magnesium und Lanthan-Magnesium. Z Metallkd. 1947;38:1–8.
7. Joseph RR, Gschneider KA. Solid solubility of magnesium in some Lanthanide metals. Trans AIME. 1965;233:2063–9.
8. Manfrinetti P, Gschneider KA. Phase equilibrium in the (0–65 at % Mg) and Gd-Mg systems. J Less Common Met. 1986;123:267–75.
9. Herchenroeder JW, Manfrinetti P, Gschneider KA. Physical metallurgy of metastable bcc lanthanide-magnesium alloy for r = la, gd, and dy. Metall Trans A. 1989;20:1575–83.
10. Giovannini M, Saccone A, Marazza R, Ferro R. The isothermal section at 500 °C of the Y-La-Mg ternary system. Metall Mater Trans A. 1995;26:5–10.
11. Guo C, Du Z. Thermodynamic assessment of the La-Mg system. J Alloy Compd. 2004;385:109–13.
12. Guo CP. Ph.D. Thesis. University of Science and Technology: Beijing, 2007.
13. Thermodata nuclear database. 2008. http://www.crct.polymtl.ca/fact/documentation/TDnucl/La-Mg.jpg. Accessed 14 Dec 2010.
14. Massalski TB. Binary alloys phase diagrams. 2nd ed. Materials Park: American Society for Metals; 1990.
15. Nayeb-Hashemi AA, Clark JB. The La-Mg (Lanthanum-Magnesium) System. Bull Alloy Phase Diagram. 1988;9:172–8.
16. Rossi A. La struttura cristallina dei composti $LaMg_3$, $CeMg_3$ e $PrMg_3$. Gass Chim Ital. 1934;64:774–8.
17. Laves F. Die Kristallstrukturen von $LaMg_2$ und $CeMg_2$. Naturwissenschaften. 1943;31:96.
18. De Negri S, Giovannini M, Saccone A. Constitutional properties of the La-Cu-Mg system at 400 °C. J Alloy Compd. 2007;427:134–41.
19. Evdokimenko VI, Kripyakevich PI. The crystal structures of magnesium-rich compounds in the system La-Mg, Ce-Mg and Nd-Mg. Kristallografiya. 1963;8:186–93.
20. Darriet B, Pezat M, Hbika A. Les alliages terre rare-magnesium riches en magnesium et leur application au stockage de l'hydrogene. Mater Res Bull. 1979;14:377–85.
21. Denys RV, Poletaev AA, Solberg JK, Tarasov BP, Yartys VA. $LaMg_{11}$ with a giant unit cell synthesized by hydrogen metallurgy: Crystal structure and hydrogenation behaviour. Acta Mater. 2010;58:2510–9.
22. Park JJ, Wyman LL. Phase relationships in magnesium alloys. National Bureau of Standards WADC-TR-57-504. 1957.
23. Rokhlin LL, Bochvar NR. The Mg-La-Ce constitution diagram. Russ Metall Metall. 1965;2:140–3.
24. Dobatkhina TV, Muratova EV, Drozdova EI. Phase composition of Mg-La-Y alloys at temperatures of 500 and 300 °C. Izv Akad nauk SSSR Metall. 1987;1:205–8.
25. SGTE. Data for pure elements. NPL report DMA(A) 195. 1989.
26. Kraus W, Nolze G. Program powder cell 2.4. FIMRT. Berlin: Germany; 2000.
27. Jriri T. Ph-D Thesis. Aix-Marseille University: France; 1994.
28. Berche A, Marinelli F, Rogez F, Record MC. Enthalpy of formation of the La-Mg intermediate phases. Thermochim Acta. 2010;499:65–70.
29. Berche A, Marinelli F, Mikaelian G, Rogez J, Record MC. Enthalpies of formation of the La-Zn compounds between 298 K and 910 K: experimental and theoritical investigations. J Alloy Compd. 2009;475:79–85.
30. Berche A, Record MC, Rogez J. Critical review of the La-Zn system. Open Thermodyn J. 2009;3:7–16.
31. Berche A, Drescher C, Rogez J, Record MC, Brühne S, Assmus W. Thermodynamic measurements in the Mg-Zn system. J Alloy Compd. 2010;503:44–9.